Supporting Information for

One-Pot Hydrothermal Synthesis of Benzalkonium-Templated Mesostructured Silica Antibacterial Agents

Viktor Dubovoy,[†] Anjani Ganti,[‡] Tao Zhang,[‡] Hassan Al-Tameemi,[#,§] Juan D. Cerezo,[#] Jeffrey M. Boyd,[#,*] and Tewodros Asefa[†,‡,*]

[†] Department of Chemistry and Chemical Biology, Rutgers, The State University of New Jersey, Piscataway, New Jersey 08854, United States

[‡] Department of Chemical and Biochemical Engineering, Rutgers, The State University of New Jersey, Piscataway, New Jersey 08854, United States

[#] Department of Biochemistry and Microbiology, Rutgers, The State University of New Jersey, New Brunswick, New Jersey 08901, United States

[§] Current Address: College of Veterinary Medicine, University of Basrah, Basrah, Iraq

1. Synthesis

Reagent grade tetraethoxysilane (TEOS), BTC® 50 solution of 50% benzalkonium chloride (BAC), and 30% aqueous ammonium hydroxide (NH_4OH) were supplied by Sigma-Aldrich (St. Louis, MO, USA), Stepan Company (Northfield, IL, USA) and Sigma-Aldrich (St. Louis, MO, USA), respectively. The distribution of alkyl chains in BAC is 50% C12, 30% C14, 17% C16, and 3% C18. All materials were used as received without any further purification. Synthesis of the MSN was carried out under mildly alkaline conditions according to the molar ratio 1 TEOS: 4 NH_4OH : 0.25 BAC : 135 H_2O. First, BAC (4.02 g), NH_4OH (11.40 g), and deionized water (56.70 g) were combined in a Teflon-lined autoclave, under magnetic stirring, to form a clear solution. Then, TEOS (5.08 g, 24.38 mmol) was added dropwise under stirring, and the mixture was subsequently heated at 80 °C for 72 h. The mixture was filtered, and a solid product was recovered. The product was then washed with copious amount of water (*ca*. 100 mL per gram of material) to remove residual reagents as well as surface-adsorbed BAC. After drying the product at 50 °C, a fluffy, white powder (BAC-SiO_2) was obtained.

For subsequent analysis and characterization experiments, some of the as-synthesized material was calcined in air at 550 °C for 6 h to remove the template, after raising the temperature from room temperature to 550 °C at a rate of 10 °C/min.

2. Characterizations

FTIR Spectroscopy. Attenuated total reflectance Fourier transform infrared (ATR-FTIR) spectroscopy was conducted on BAC-SiO_2 and lyophilized BAC samples. The ATR-FTIR spectra (650-4000 cm^{-1} with 4 cm^{-1} resolution) were collected using Spectrum 2000 FTIR spectrometer, (PerkinElmer, Waltham, MA, USA) equipped with a KBr beam splitter, DTGS detector, and single-bounce diamond ATR crystal.

N_2 Porosimetry. The surface areas, pore sizes and pore volumes of the materials were determined after obtaining N_2 adsorption-desorption isotherms using a Tristar 3000 instrument (Micromeritics Norcross, GA, USA) equipped with FlowPrep 060 Sample Degas System. Prior to N_2 sorption experiments, the samples were de-gasified for 8 h at 80 °C under a N_2 atmosphere. The specific surface areas were calculated by using the Brunauer-Emmett-Teller (BET) method. The pore sizes and pore size distributions were calculated from the isotherms according to the Barrett-Joyner-Halenda (BJH) method. From the amount of N_2 adsorbed at a relative pressure (P/P_0) of 0.99, the total pore volume of the material was obtained.

Static Light Scattering (SLS). The size distribution of the BAC in aqueous solution was measured by the static light scattering technique. An aliquot of the fresh solution was transferred to a polystyrene cuvette prior to analysis.

Synchrotron-based Small-Angle X-Ray Scattering (SAXS). The SAXS measurements were performed at the 12-ID-B beamline of the Advanced Photon Source (APS) at Argonne National Laboratory, using 13.3 Kev X-ray energy source that has a wavelength of 0.9322 Å. The SAXS data were collected with a Pilatus 2 M detector (DECTRIS Ltd.), and the cutoff energy was set as 10 Kev to eliminate the possible fluorescence background. A beam with a size with 0.1 × 0.2 mm^2 and an exposure time of 1s was used for the measurements. The sample-to-detector distance was *ca.* 2 m, and the scattering vector (q) range covered 0.004 - 0.9 A^{-1}. The 2-D SAXS patterns were fully corrected, reduced to 1-D intensity versus q profiles, and background subtracted, using the software package at the beamline.

Thermogravimetric Analysis (TGA). The amount of BAC incorporated in the mesostructured material was calculated by thermogravimetric analysis (TGA) using a TGA 7 Thermogravimetric

Analyzer (PerkinElmer, Waltham, MA, USA). The analysis was carried out in platinum crucibles over a temperature range of 50-550 °C at a heating rate of 10 °C /min.

Transmission Electron Microscopy (TEM). Sample preparation entailed suspending the sample in ethanol, dropping onto a holey copper grid, and allowed to air-dry in room temperature. The electron microscopy experiments were performed using a JEOL 2010F microscope operated at 197 kV. The spatial resolution of the microscope in the high resolution (HRTEM) mode is ~1.4 Å. The fast Fourier transform of the HRTEM images generates spots which correspond to crystallographic periodic arrangements of atomic planes. These spots were also used as filters to remove background noise from the high-resolution images. All HRTEM images were analyzed using Gatan Digital Micrograph software.

Differential Scanning Calorimetry (DSC). Differential scanning calorimetry was conducted on a TA DSC Q20 equipped with a TA refrigerated cooling system.

Small-Angle X-Ray Diffraction (SAXRD). The X-ray scattering from the sample was obtained by using a Brüker VÅNTEC-500 area detector equipped with a Brüker FR571 rotating-anode X-ray generator operating at 40 kV and 50 mA. The diffraction system was equipped with a 3-circle Azlan goniometer, but the sample was not moved during X-ray data collection. The system used 0.5 mm pinhole collimation and a Rigaku Osmic parallel-mode (*e.g.*, primary beam dispersion less than 0.01 deg in 2θ) mirror monochromator (Cu Kα; λ = 1.5418Å). Data were collected at room temperature (20 °C) with a sample to detector distance of 26.2 cm. Spatial calibration and flood-field correction for the area detector were performed at this distance prior to data collection. Images with 2048 x 2048 pixel were collected at the fixed detector (2θ) angle of 50 ° for 3 min with ω step of 0.00 deg. For the intensity versus 2θ plot, a 0.02 ° step, bin-normalized χ integration was performed on the image shown below with settings $0 < 2\theta < 13$ ° and $-180 < \chi < 180$ °. Data collection and rocking curve creation were done with Brüker GADDS v.4.1.51 (2015). Data display and graphics were done with MDI JADE7 v.7.0.6 (2004).

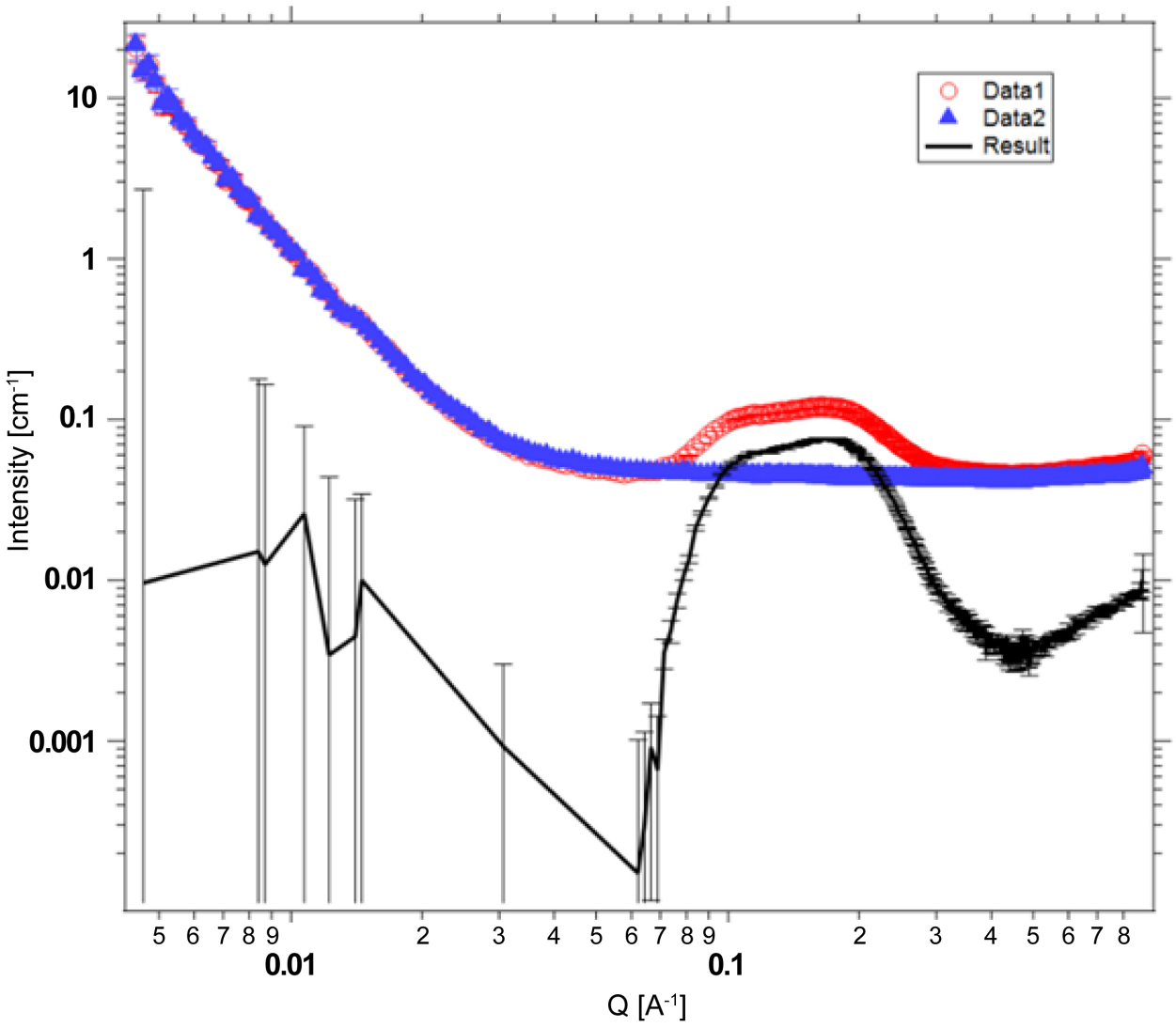

Figure S1. Synchrotron-based SAXS of aqueous BAC/NH_4OH solution prior to TEOS addition (red) with its corresponding curved fit (blue) and their difference (black).

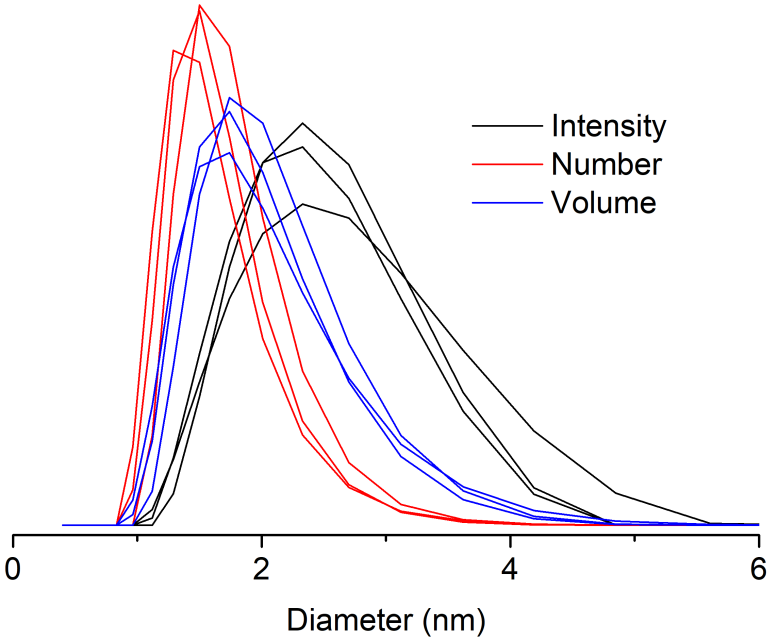

Figure S2. Static light scattering (SLS) pattern of aqueous BAC/NH_4OH solution prior to the addition of TEOS demonstrating scattering intensity versus diameter.

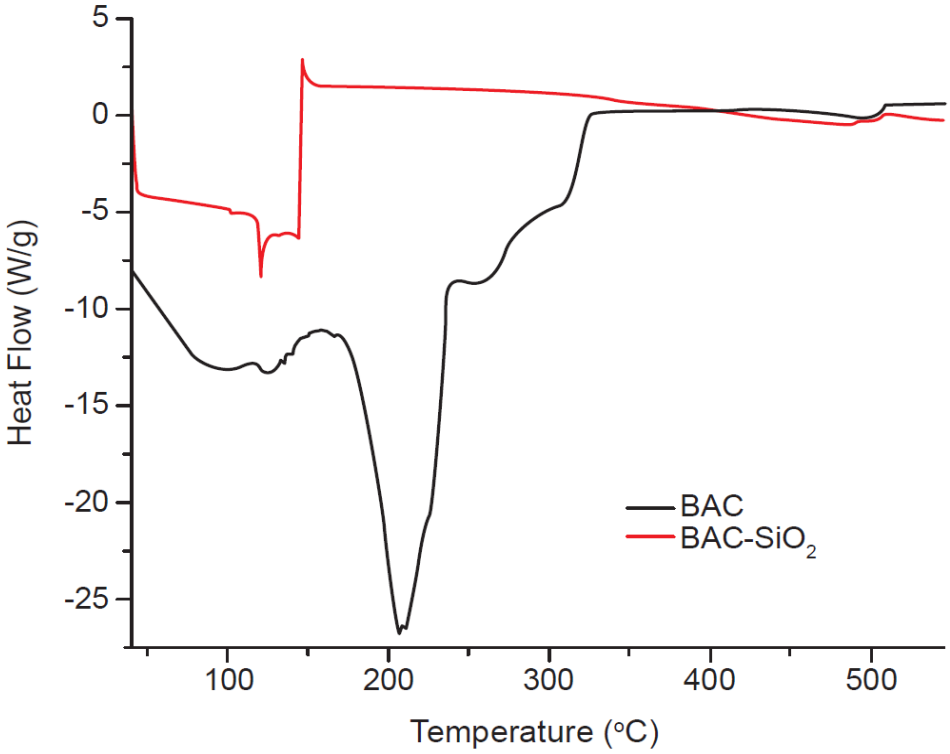

Figure S3. Differential scanning calorimetry (DSC) plots of BAC and BAC-SiO_2. The result shows the decomposition of BAC takes place at lower temperature when it is in form of BAC-SiO_2 than when it is in pure form. This result is consistent with the major step of thermal degradation observed in TGA graph for BAC-SiO_2 versus that of pure BAC (Figure 2b). DSC results obtained for the materials here further showed that the predominant endothermic peak for BAC-SiO_2 and BAC occurred at 120-140 °C and 185-230 °C, respectively. A decrease in thermal degradation onset within the silica framework can be explained by the fact that pure BAC exhibits more crystallinity than that of the amorphous BAC phase within the framework.

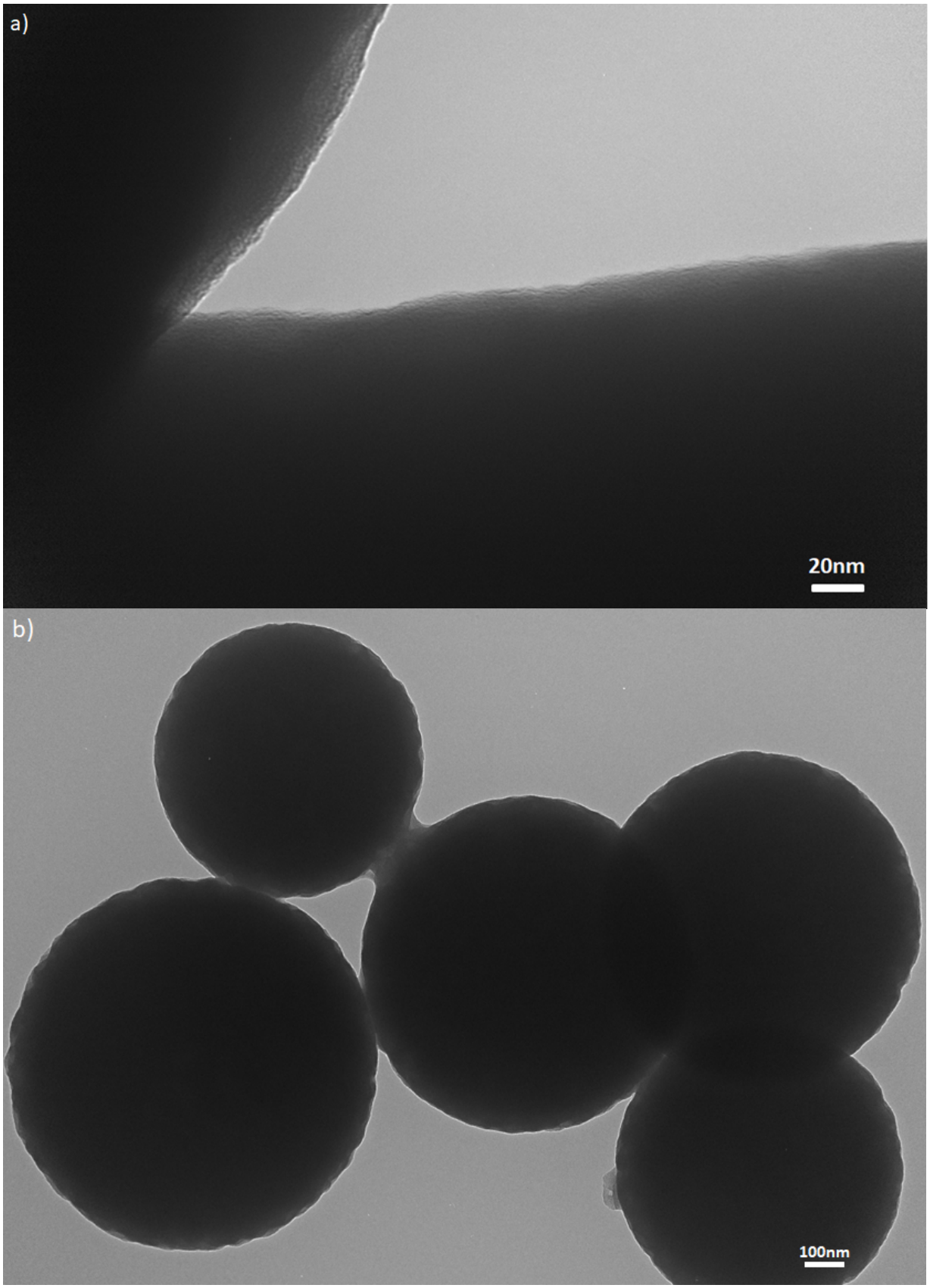

Figure S4. High (a) and low (b) magnification transmission electron microscope (TEM) images of as-synthesized BAC-SiO_2 microparticles. The sizes of the particles were largely in between 650-850 nm.

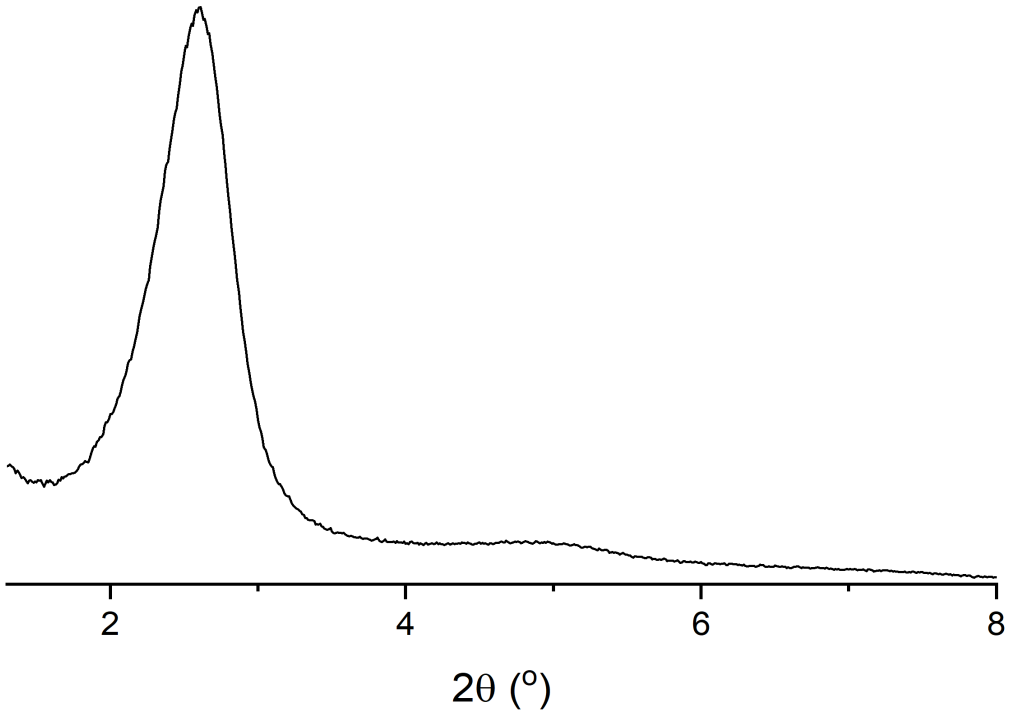

Figure S5. Small-angle X-ray diffraction (SAXRD) pattern of as-synthesized BAC-SiO_2.

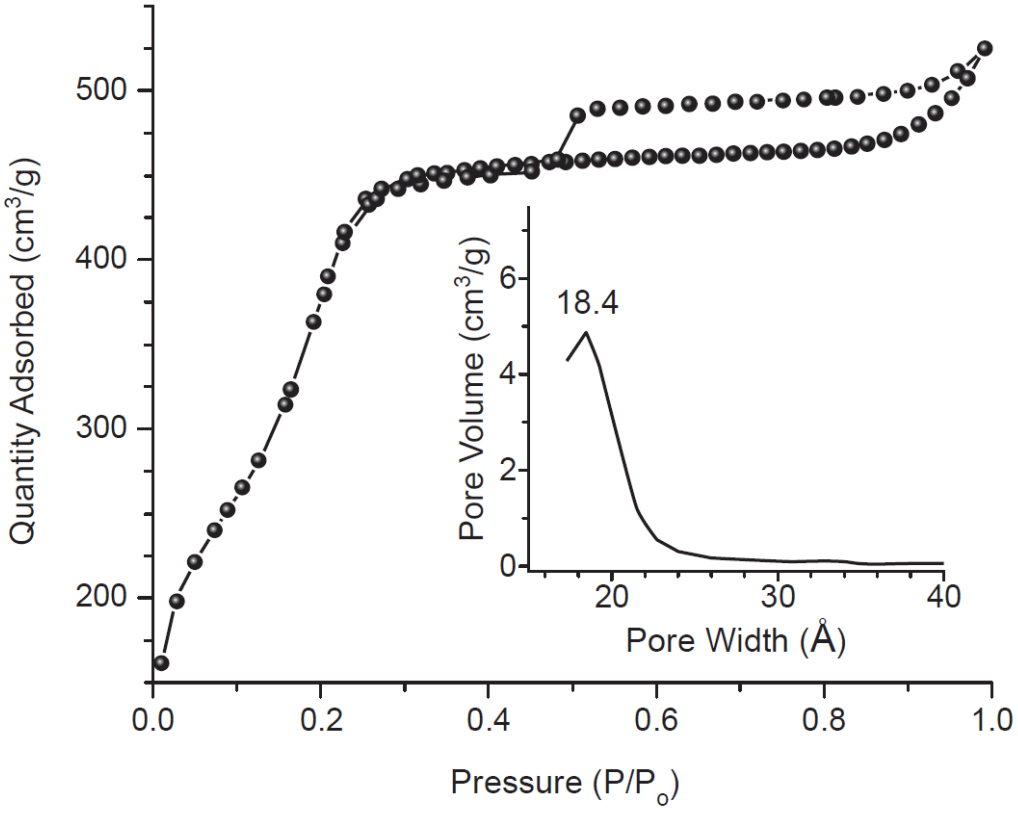

Figure S6. Nitrogen (77 K) sorption isotherms of calcined BAC-SiO_2 and pore size distribution shown in inset.

3. Drug Release Studies

The release of BAC from BAC-SiO_2 under static condition at room temperature was investigated at different pH conditions: 1) phosphate-buffered saline (PBS) solution pH 7.4 and 2) PBS solutions acidified to pH 4.0, 5.0, and 6.5 with HCl. Calibration curves were plotted by measuring the UV-Vis spectroscopy of pure BAC in the corresponding solutions. Specifically, 400 mg of BAC-SiO_2 was suspended in 50 mL of dispersion medium. The solution was centrifuged at prefixed time intervals, and a 1 mL aliquot of the supernatant was taken using a pipette and analyzed for BAC content at λ_{max} of 262 nm. The region between 240 and 280 nm exhibited three peaks in UV-Vis, which is consistent with UV-Vis of other quaternary ammonium surfactants.[1] The analyzed supernatant was then returned to the solution. This process was repeated at different intervals of time until no further substantial release of BAC was observed. The absorption intensity was plotted as a function of time using a Lambda 850 UV/Vis Spectrometer (PerkinElmer, Waltham, MA).

BAC release studies at low pH values (*e.g.*, 1-2) were unsuccessful and a great deal of effort was directed towards identification of an appropriate release medium, as well as BAC concentration measurement. *In situ* concentration measurements using UV-Vis spectrometer or conductivity instruments failed due to interference from the particles or inability to correlate the measurements to the concentration of free BAC molecules, respectively. In fact, two centrifugation steps were required to implement prior to UV-Vis measurements to minimize the interference from suspended particles. It is proposed herein that the dispersion of cleaved framework particles with a size on the order of UV-Vis wavelength (*i.e.*, 300-800 nm) caused elastic scattering and interfered with the UV-Vis measurements. This interference of silica nanoparticles was also reported elsewhere.[2] Incorporation of several consecutive centrifugation steps was necessary to accurately measure the concentration at λ_{max} = 262 nm. BAC exhibits three predominant UV-Vis absorption peaks in the range of 240-280 nm (Figure S6) which are proposed herein to originate from benzene's $\pi \rightarrow \pi^*$ electronic excitations. The λ_{max} = 262 nm is reasonable if considering λ_{max} of toluene at 261 nm with a bathochromic effect caused by the apparently weak inductive effect of the relatively distant cationic substituent.

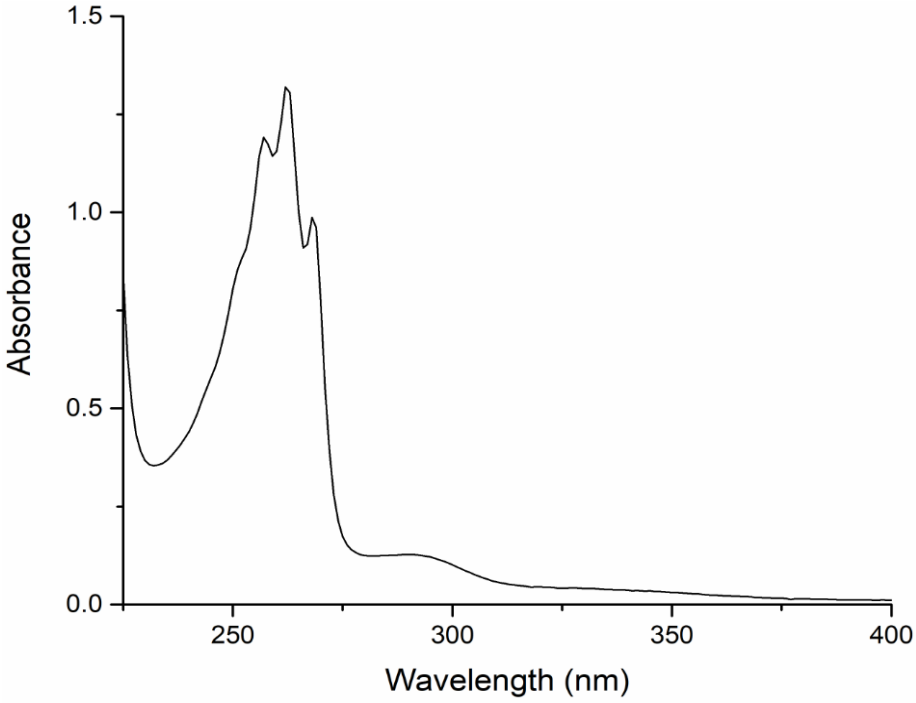

Figure S7. UV-Vis spectrum of BAC in a quartz cuvette (shown is a portion of the 200-800 nm scan).

The drug loading capacity was then computed to a value of x g/g using the following equation:

$$\boldsymbol{Drug\ loading\ capacity} = \frac{\boldsymbol{mass\ of\ drug\ in\ the\ MSNs}}{\boldsymbol{mass\ of\ drug-loaded\ MSN}} \qquad \text{Eqn. 1}$$

4. Kinetics Analysis

Kinetic analysis was conducted via Power law model, which is used widely in the literature.[3-6]

$$\frac{M_t}{M_\infty} = kt^n$$

$$\rightarrow \log\frac{M_t}{M_\infty} = \log kt^n$$

$$\rightarrow \log\frac{M_t}{M_\infty} = \log k + \log t^n$$

$$\rightarrow \log\frac{M_t}{M_\infty} = \log k + n\log t$$

$$\rightarrow \log\frac{M_t}{M_\infty}(y) = \log k\ (constant\ b) + n\log t\ (x); [y = nx + b]$$

$\mathbf{M_t/M_\infty}$ is a fraction of drug released at time $\boldsymbol{t}$, $\boldsymbol{k}$ is the release rate constant and $\boldsymbol{n}$ is the release exponent. The value of $\boldsymbol{n}$ is used to determine the release mechanism; $\boldsymbol{n}$ and $\boldsymbol{k}$ can be calculated from graph's slope and y-intercept, respectively.

Table S1. Analysis of kinetic data for BAC desorption.

Release Media	pH	log (M_t/M_∞) vs. log (*t*)	*n*	*R*
PBS	4.0	y = 0.183x – 0.69	0.183 ± 0.003	0.99
PBS	5.0	y = 0.134x – 0.67	0.134 ± 0.020	0.96
PBS	6.5	y = 0.141x – 0.55	0.141 ± 0.025	0.94
PBS	7.4	y = 0.717x – 0.41	0.717 ± 0.144	0.92

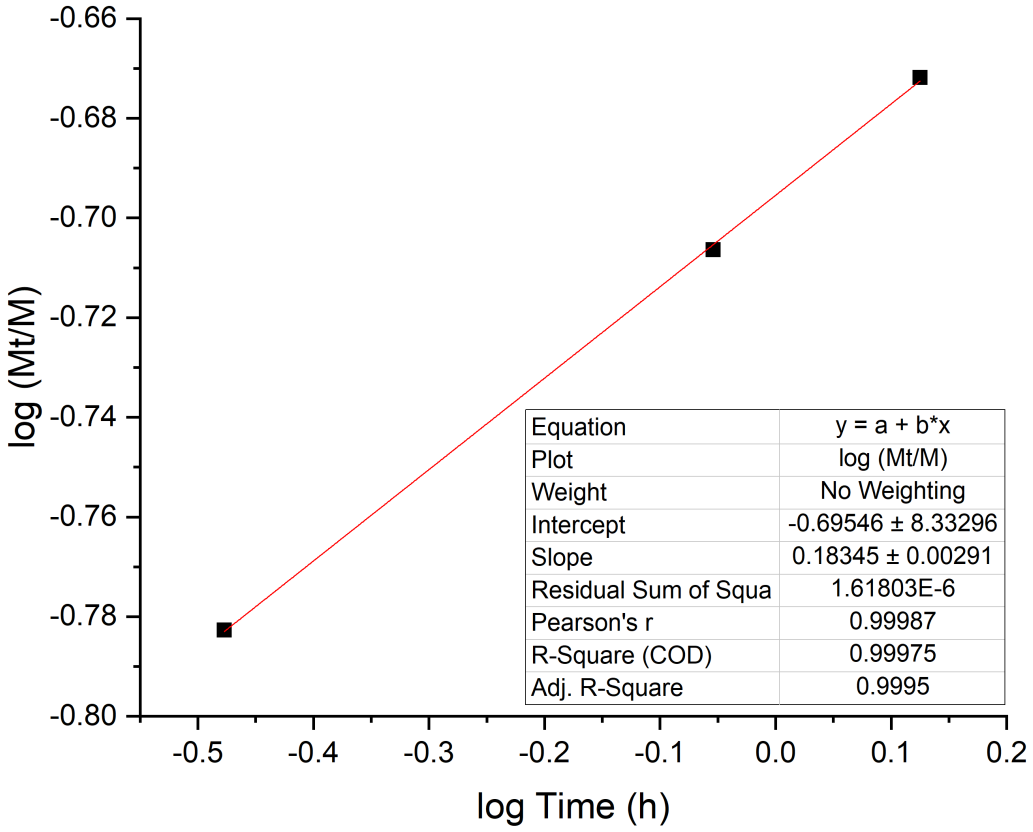

Figure S8. Logarithmic variation of BAC fraction released over time in PBS pH 4.0.

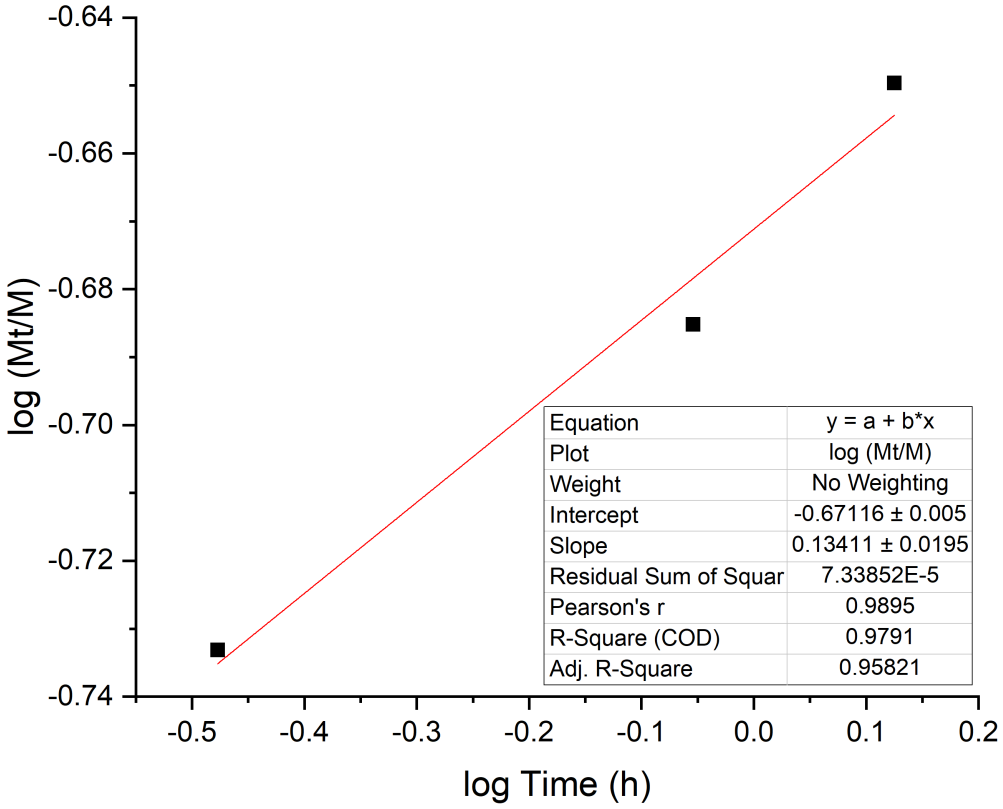

Figure S9. Logarithmic variation of BAC fraction released over time in PBS pH 5.0.

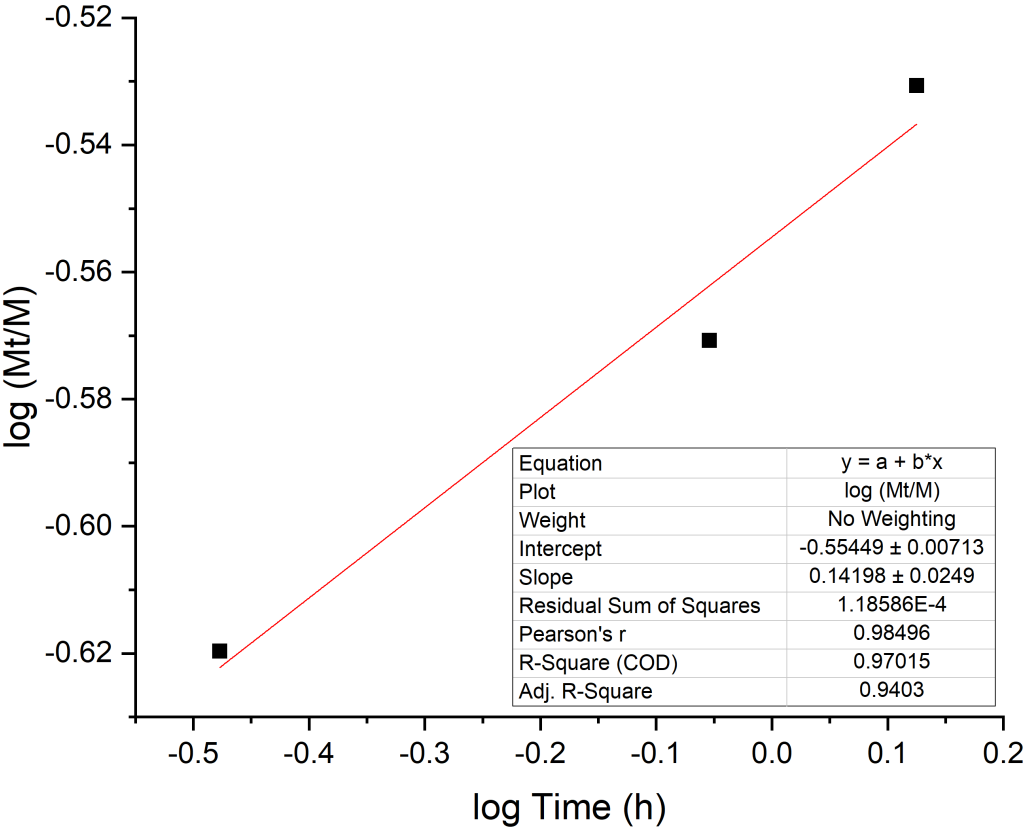

Figure S10. Logarithmic variation of BAC fraction released over time in PBS pH 6.5.

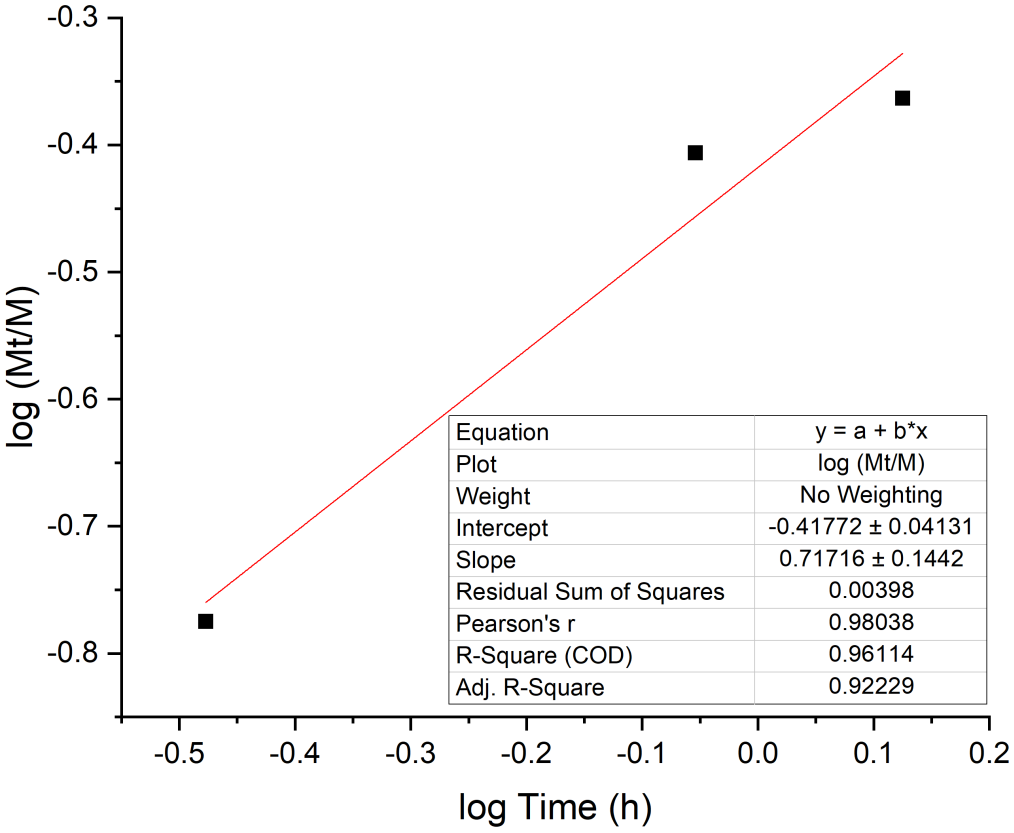

Figure S11. Logarithmic variation of BAC fraction released over time in PBS pH 7.4.

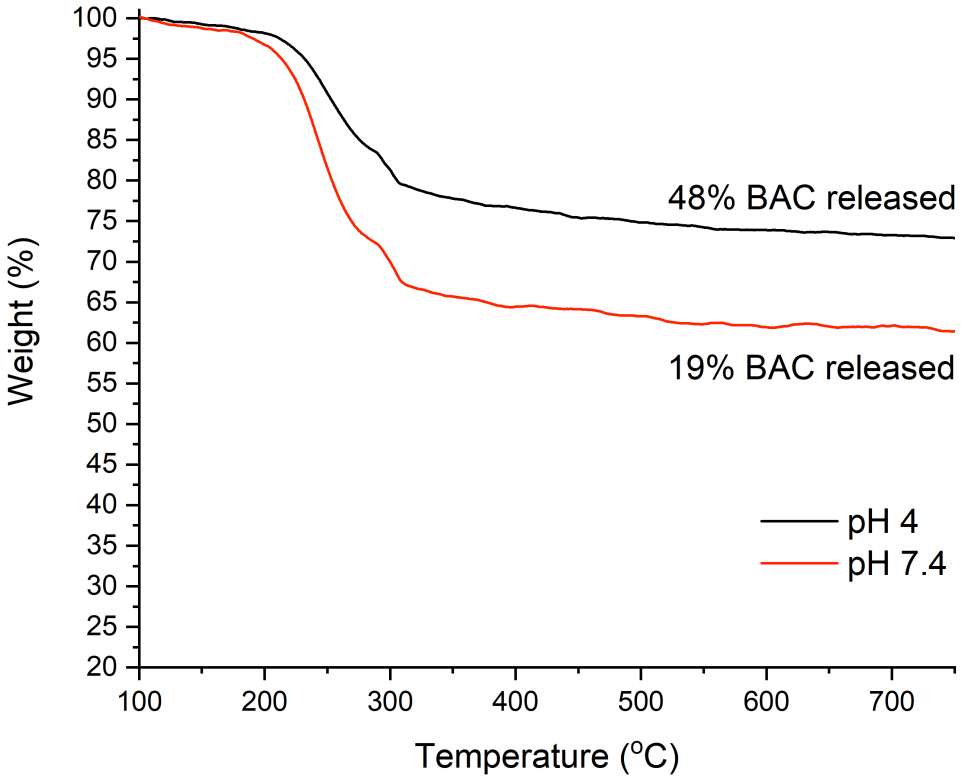

Figure S12. TGA curves of BAC-SiO_2 material after letting the sample consecutively release BAC in seven fresh solutions at pH 4 and pH 7.4. Each time, the sample is kept in the solution for 24 h. The result indicates that the BAC-SiO_2 releases 48% and 19% of BAC. These results are also in line with other experimental results obtained earlier. For example, after 10 days of constant stirring of BAC-SiO_2 in PBS solutions of pH 4 and pH 7.4, about 15% and 7% of BAC, respectively, are released from the material. The data and kinetic analysis suggest that hydronium ions (H_3O^+) play an important role and enhance the drug release (*e.g.,* pH 7.4 shows *ca.* 2% release of BAC while pH 4 shows *ca.* 8% release of BAC after 2.5 days). Experiments also demonstrated that after releasing *ca.* 8% of the total drug content, the material releases another 5% BAC once placed in a fresh solution. The data suggest that the release continues until reaching an equilibrium between BAC inside the mesoporous silica vehicle and free BAC in the solution. Decreasing the pH shifts the equilibrium in the direction of free BAC. Therefore, in the dynamic scenario where fresh solution constantly flows through BAC-SiO_2, the majority of the BAC in the material can be ultimately released, as also demonstrated by the TGA graphs above.

4. Microbiological Assays

Cultures of *Staphylococcus aureus* USA300_LAC and *Salmonella enterica* serovar typhimurium LT2 were grown for 18 hours in 75 mL of Mueller-Hinton (Sigma-Aldrich) medium in 250 mL flasks. Broth cultures were grown at 37 °C with a shake speed of 200 RPM in 250 mL flasks. *S. enterica* and *S. aureus* were individually diluted in triplicate into flasks containing 30 mL or 100 mL of Mueller-Hinton broth to an optical density (A_{600}) of 0.1, respectively. Subsequently, bacteria were combined with vehicle control, BAC-SiO_2, BAC, or SiO_2. At various times after addition (*i.e.,* 0, 3, and 6 hours), bacteria were removed from the flasks, serial diluted using sterile phosphate buffered saline (PBS) solution, using sterile microtiter plates. Subsequently, 5 μL of each dilution was dropwise plated onto solid tryptic soy medium (MP biomedical). The plates were incubated at 37 °C for 18 hours before the number of viable bacteria was enumerated by counting the number of colony-forming units (CFU).

5. Additional Discussion on the Bactericidal Property of BAC-SiO_2

We have also checked whether or not possible residual synthetic reagents, specifically the alkaline catalyst, may be responsible for the extraordinary antibacterial effect exhibited by the material in question (*i.e*., BAC-SiO_2). Based on the experiments we have conducted (below), we were able to confirm that residual alkaline catalyst (NH_4OH), if any, does not have a significant effect on the pH nor on the growth rate of *S. aureus* and *S. enterica*.

The concentration of BAC-SiO_2 used for antimicrobial assays illustrated in Figure 3b-c ranged between 0-200 mg/L. Accordingly, aqueous solutions of BAC-SiO_2 were prepared in 0.1 M NaCl to evaluate the effect of BAC-SiO_2 material on the pH of the solution. Solutions containing 0, 30, 60, 120, and 200, and also 400 mg/L of BAC-SiO_2 were freshly prepared. The last concentration was intentionally included to make sure that even higher concentration do not affect the microbes. The measured pH of 0.1 M NaCl and the BAC-SiO_2 solutions was 6.10 and 5.65 ± 0.22, respectively. The reduction in pH value upon addition of BAC-SiO_2 suggests that the as-synthesized material makes the solution slightly acidic. It is noteworthy that a strong alkaline effect was not observed in this experiment, which would indicate a reasonable amount of excess acid must be present in the solution due to hydrolysis processes. Notably, based on the reagents used during the synthesis, there are only three/four major species that can contribute to pH in these solutions:

1. Deprotonation of Si-OH and hydrolysis of Si-O-Si moieties;
2. Possible residual NH_3 and/or NH_4OH; and
3. Hydrolysis of benzalkonium (RNH_4^+) ions (which leads to acidic solution as per the following two reactions: $RNH_4^+ + H_2O <==> RNH_4OH + HCl$ and $HCl + H_2O \rightarrow H_3O^+(aq) + Cl^-(aq)$)

In this case, since the pH is < 7.00 and the pH is lower than that of the pure solvent environment, we can safely say that the acidic species (formed due to benzalkonium hydrolysis, Si-OH deprotonation) overpower the alkaline species (*e.g.*, NH_3, Si-O-Si) in terms of pH effect. Since the antimicrobial assays were carried out in buffered media, we expect a similar pH effect, but to a lesser extent due to the buffering effect.

To be quite sure, we have performed some additional biological control experiments using NH_4OH. At the concentrations examined, NH_4OH has no effect on *S. aureus* or *S. enterica* growth (Figures S13 below) and the viability of the microbes (Figure S14 below). As illustrated in the figures, the microbial growth and proliferation rates cannot be discerned from the samples containing 30 or 200 mg/L NH_4OH and the blank control. The concentrations of 30 and 200 mg/L NH_4OH were chosen as to demonstrate that even if 100% of the BAC-SiO_2 consisted of NH_4OH, it would not demonstrate any bacteriostatic or bactericidal effect.

These results are also in line with those previously reported in the literature. The cytotoxicity of ammonia was evaluated on a variety of biological organisms. It was demonstrated that in contrast to animal and plant cells, ammonia was not toxic for various bacteria such as *C. glutamicum*, *E. coli*, and *B. subtilis* even in molar concentrations.[7]

So, based on these results, we still believe that the reason for the as-synthesized BAC-SiO_2 to show a significant antibacterial effect than free BAC, despite the former can release less BAC into the solution than the latter, is simply because the as-syn BAC-SiO_2 helps make the BAC more accessible to the microbes better than free BAC can. It is possible that releasing the BAC in localized manner on the cell surface may result in more efficacy/greater killing. This possibility is not unprecedented. It is quite known that the biological activities (such as antibacterial effect, anticancer effect, etc.) of many small molecules and ions get enhanced by nanoparticles. For example, related bioactive-loaded silica-based nanoporous materials called xerogels are reported to show higher antibacterial potency than the same amount of free bioactive molecules.[8,9] This is also true anticancer drugs against and cancer cells, as we and others had previously reported.[10]

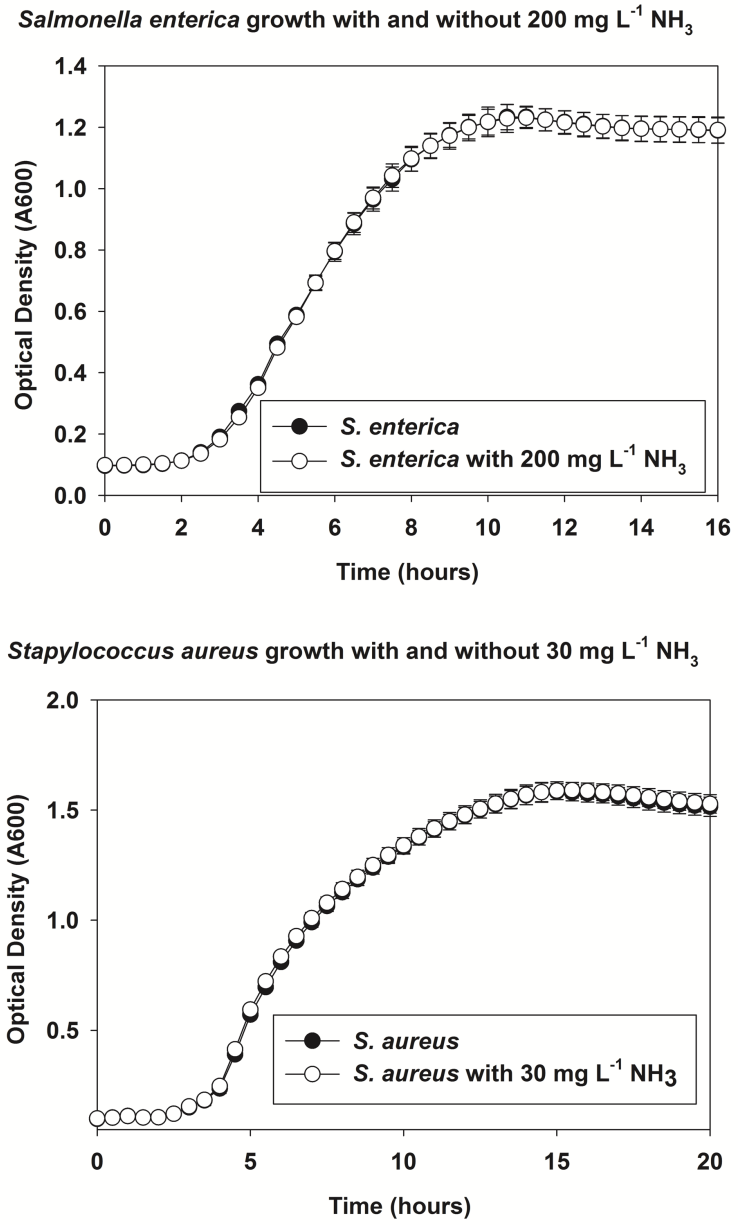

Figure S13. Growth analyses of *S. enterica* (top panel) and *S. aureus* (bottom panel) in the presence of NH_4OH. Data represent growth traces. The concentrations of NH_4OH was and 200 mg L^{-1} and 30 mg L^{-1} for *S. enterica* and *S. aureus,* respectively. Experiments were conducted in triplicate and error bars represent standard deviations. Errors bars are shown for all data points, but are sometimes too small to visualize.

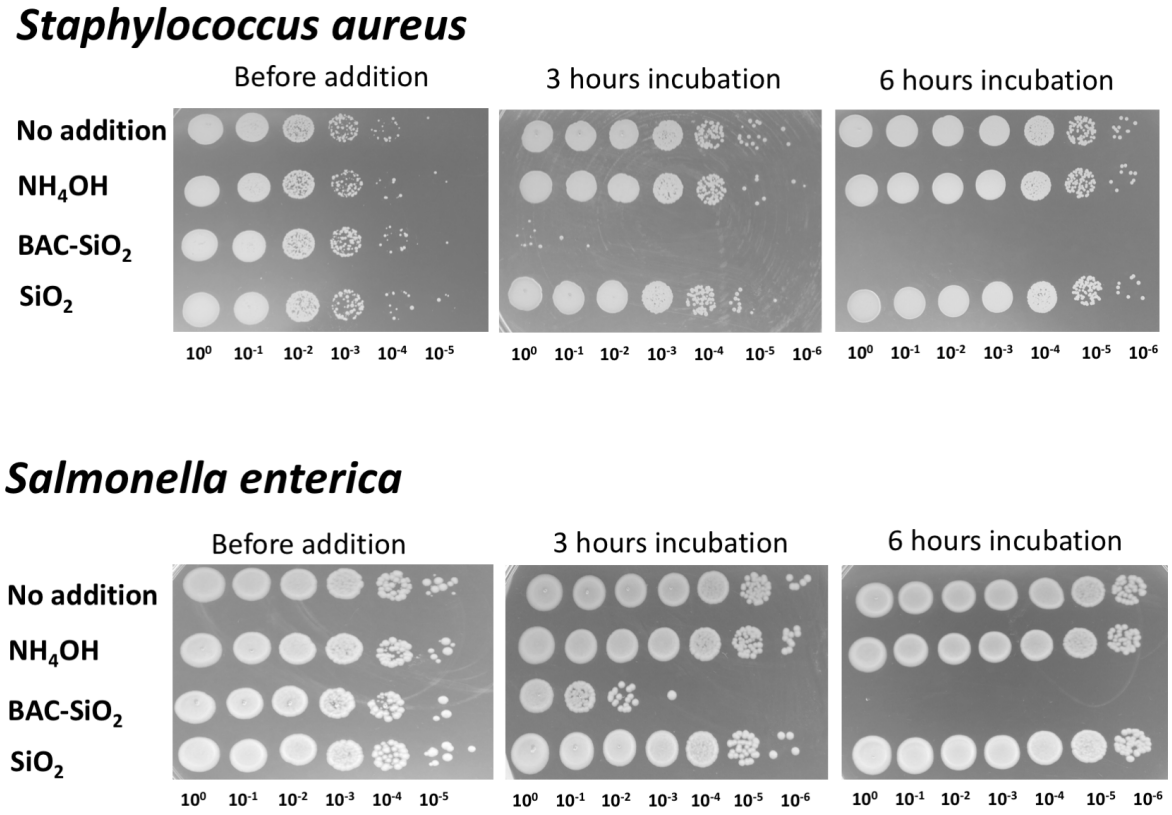

Figure S14. Supplemental Figure X. Time- and dose-dependent killing of *S. aureus* and *S. enterica* by NH_4OH, BAC-SiO_2, or SiO_2. The concentrations of all additions were 30 mg L^{-1} and 200 mg L^{-1} for *S. aureus* and *S. enterica*, respectively. Photograph display drop plates containing 10-fold serial dilutions (right to left: 10^0 to 10^{-6}) of treated cultures.

5. References

(1) Dement'eva, O. V.; Rudoy, V. M. *RSC Adv.* **2016,** *6*, 36207-36210.

(2) Selvaggi, R.; Tarpani, L.; Santuari, A.; Giovagnoli, S.; Latterini, L. *Appl. Catal. B* **2015,** *168*, 363-369.

(3) Dash, S.; Murthy, P. N.; Nath, L.; Chowdhury, P. *Acta Pol. Pharm.* **2010,** *67*, 217-23.

(4) Dement'eva, O. V.; Senchikhin, I. N.; Kartseva, M. E.; Ogarev, V. A.; Zaitseva, A. V.; Matushkina, N. N.; Rudoy, V. M. *Colloid J.* **2016**, *78*, 586-595.

(5) Fidalgo, A.; Lopez, T. M.; Ilharco, L. M. *J. Sol-Gel Sci. Technol.* **2009**, *49*, 320-328.

(6) Costa, P.; Sousa Lobo, J. M. *Eur. J. Pharm. Sci.* **2001,** *13*, 123-133

(7) Muller, T.; Walter, B.; Wirtz, A.; Burkovski, A. *Curr Microbiol.* **2006**, *52*, 400-406.

(8) Seleem, M. N.; Munusamy, P.; Ranjan, A.; Alqublan, H.; Pickrell, G.; Sriranganathan, N. *Antimicrob. Agents and Chemother.* **2009**, *53*, 4270-4274.

(9) Miller et al., Inorganic Nanoparticles Engineered to Attack Bacteria, *Chem. Soc. Rev.* **2015**, *44*, 7787-7807.

(10) Tao, Z.; Toms, B.; Goodisman, J.; Asefa, T. *ACS Nano* **2010**, *4*, 789-794.